Supporting Information for

Alginate as a Green Inhibitor of Barite Nucleation and Crystal Growth

Xi Geng,[1‡] Ricardo D. Sosa,[1‡] Michael A. Reynolds[2]*, Jacinta C. Conrad[1]*, Jeffrey D. Rimer[1]*

[1] Department of Chemical and Biomolecular Engineering, University of Houston, Houston, Texas 77204, United States

[2] Shell Exploration & Production Company, Royal Dutch Shell, plc, Houston, TX 77082, USA

‡ These authors contributed equally to this work
* Correspondence sent to:
Mike.Reynolds@shell.com, jcconrad@uh.edu, and jrimer@central.uh.edu

Table of Contents

List of Supplementary Figures

Supporting Figures

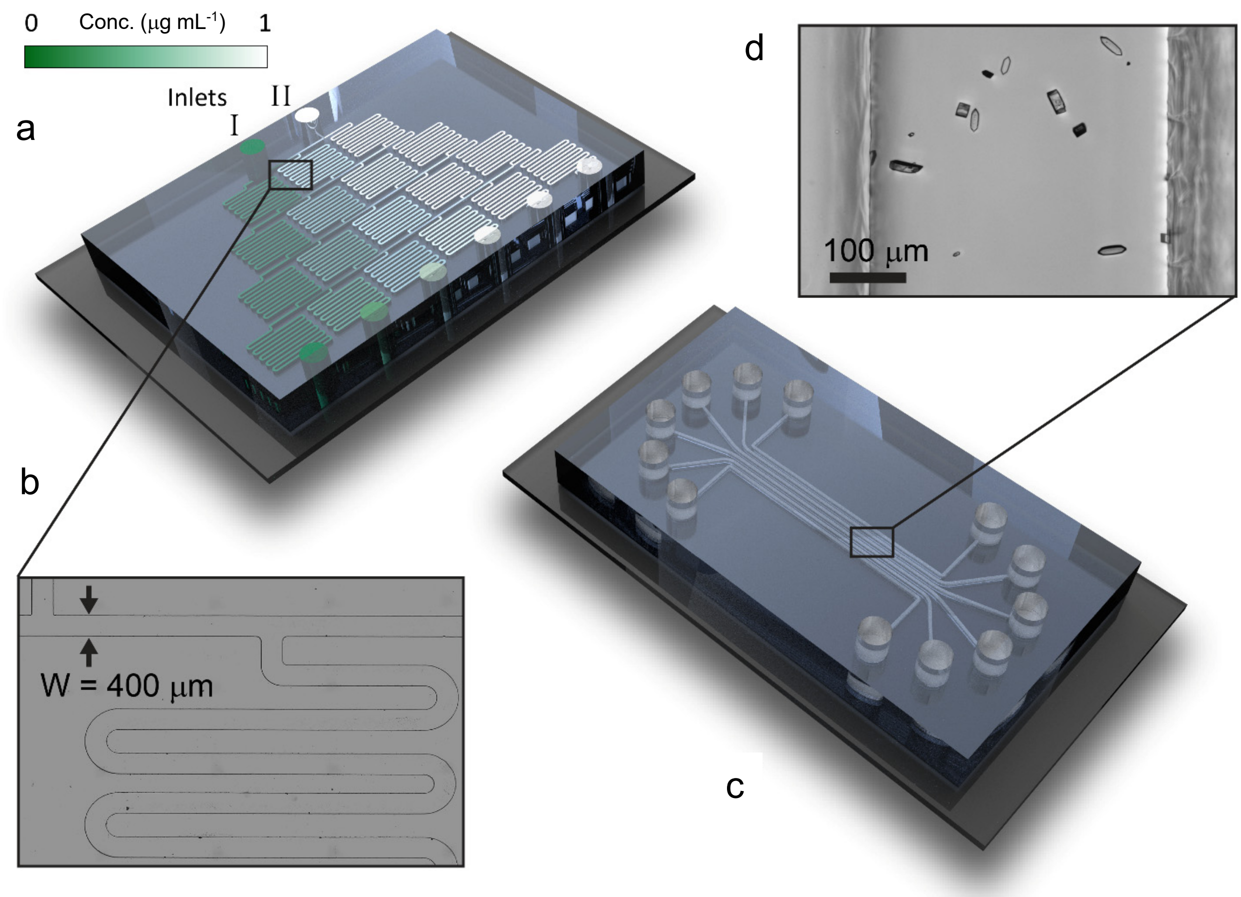

Figure S1. Microfluidic platform used in this study. (a) Three-dimensional rendering of the gradient generator. The color bar represents the concentration of a given inhibitor in solution: green indicates a concentration of 0 μg mL^{-1}, and white indicates a concentration of 1 μg mL^{-1} for modifier studies. The cross-sectional area of all channels is 200 × 400 μm^2. For modifier studies, growth solution is flowed into inlet I and growth solution with the desired amount of modifier at supersaturation $S = 7$ is flowed into inlet II. (b) Optical micrograph of the microchannels in the gradient generator, indicating the width of the microchannel is 400 μm. (c) The gradient generator feeds into a microfluidic device for seeded growth and visualization of barite crystals. The device consists of six microchannels of cross-sectional area 200 × 400 μm^2 and length 5 cm. (d) Representative optical micrograph of the straight microchannels in the second device containing barite seed crystals of 35 μm average length. This figure is reproduced from reference 52 in the manuscript (Sosa et al., *Lab on Chip*, 2019).

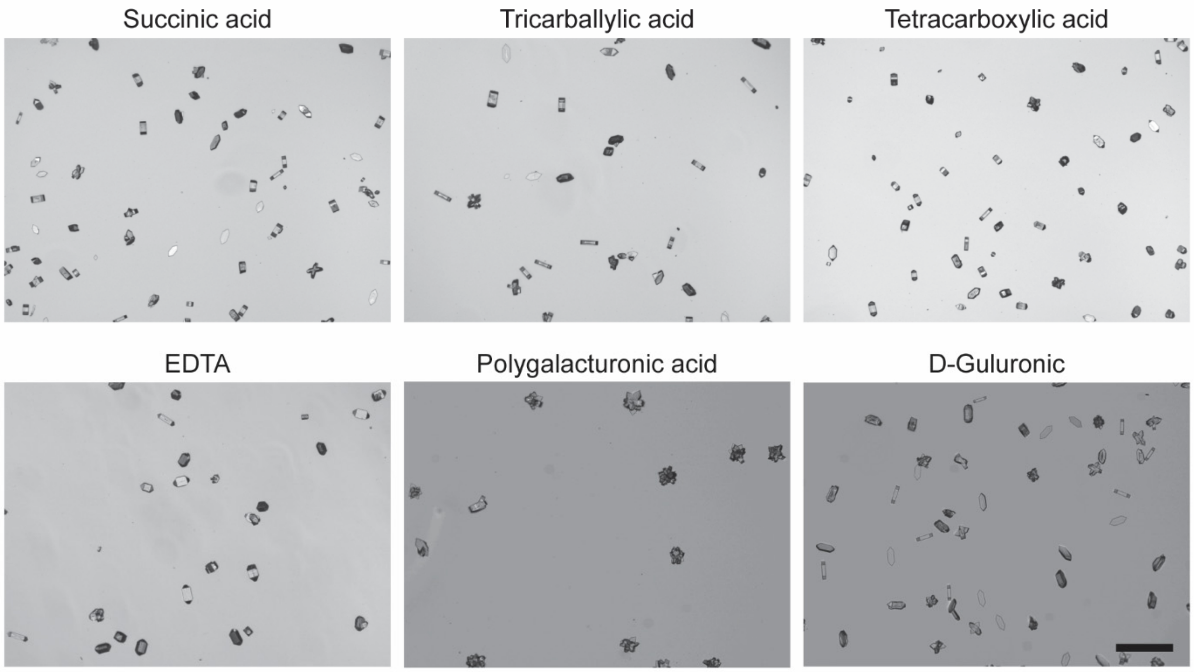

Figure S2. Representative optical images of barite crystals synthesized in the presence of 1 μg mL^{-1} of each additive with an initial supersaturation S = 10 under quiescent conditions at room temperature (21.0 ± 0.5 °C) for 24 h. Scale bar equals 100 μm.

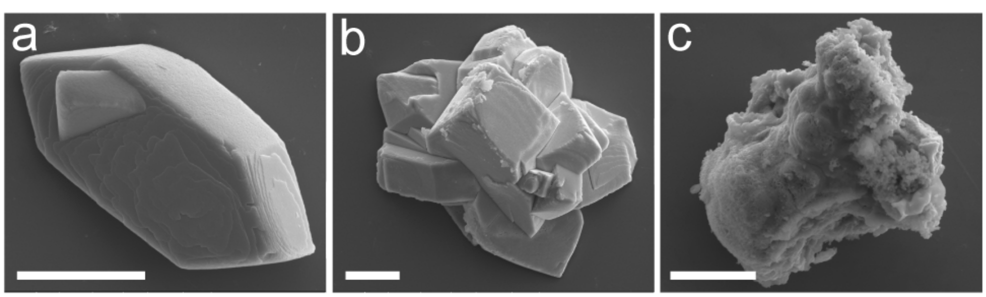

Figure S3. (a) SEM images of barite crystals synthesized under quiescent conditions in the presence of (a) 0.2, (b) 0.4, and (c) 0.8 μg mL^{-1} alginate with an initial supersaturation S = 10 under quiescent conditions at room temperature (21.0 ± 0.5 °C) for 24 h. Scale bars equal 10 μm.

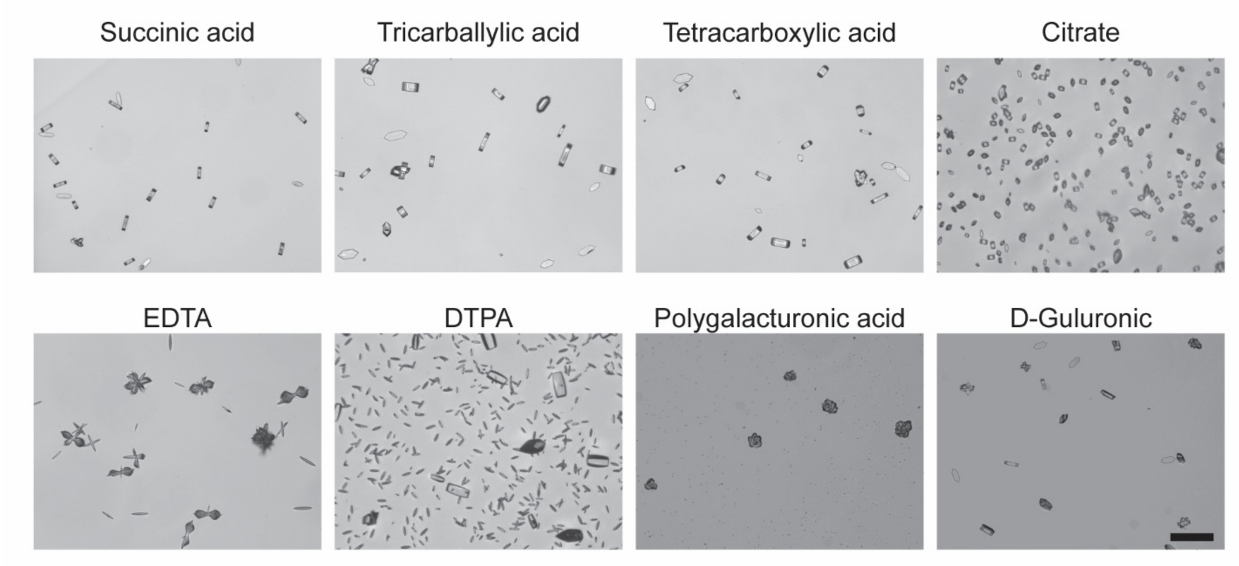

Figure S4. Representative optical images of barite crystals synthesized in the presence of 10 μg mL^{-1} of each additive with an initial supersaturation ratio S = 10 under quiescent conditions at room temperature (21.0 ± 0.5 °C) for 24 h. Scale bar equals 100 μm.

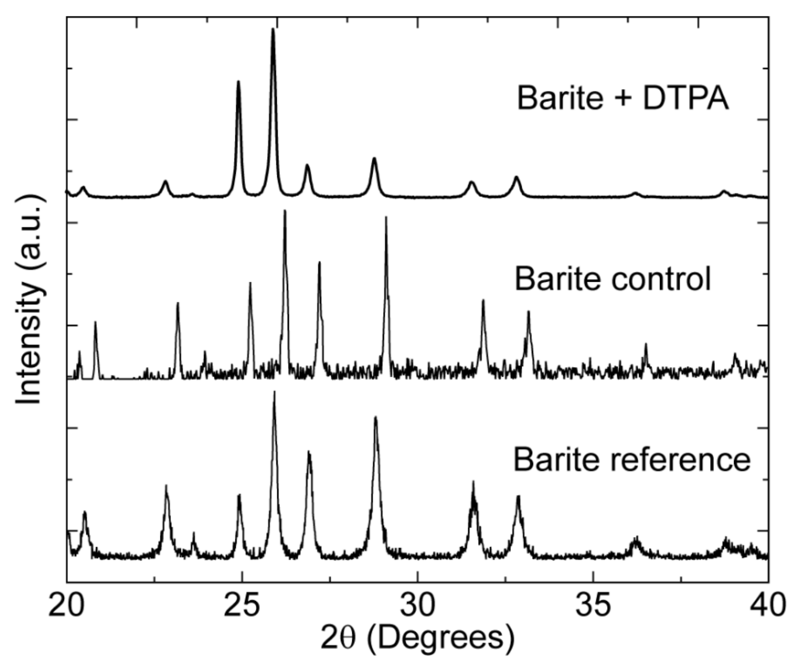

Figure S5. Powder XRD patterns of as-synthesized barite crystals from bulk assays in the presence and absence of 10 mg mL^{-1} DTPA and a reference sample from the ICDD PDF-2 2013 database. Bulk assays were conducted under quiescent conditions at room temperature (21.0 ± 0.5 °C) for 24 h with initial supersaturation ratio S = 10.

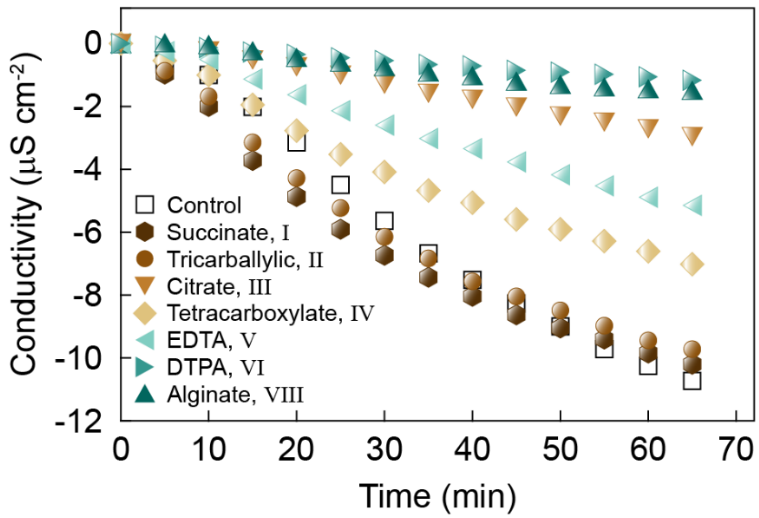

Figure S6. Representative desupersaturation curves tracking the conductivity of barite growth solutions (S = 10) at ambient temperature (21.0 ± 0.5 °C) during bulk assay synthesis while stirring (400 rpm). A linear regression is performed on the first 40 min of each experiment to report the depletion rate of growth solutes from the bulk.

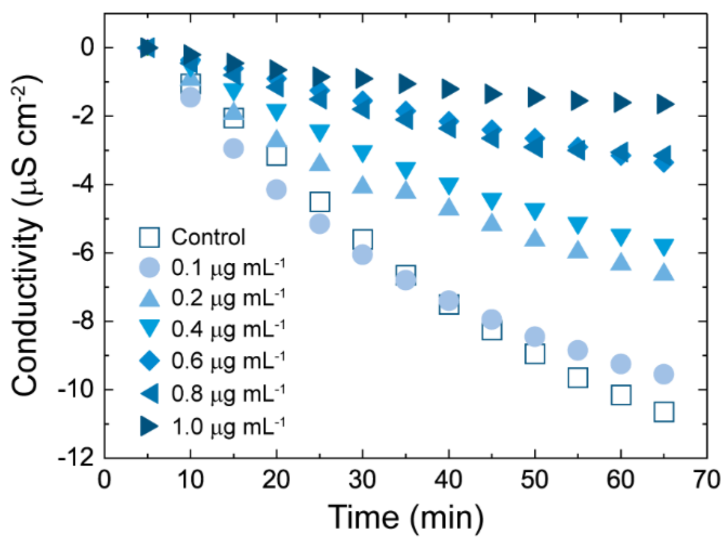

Figure S7. Representative desupersaturation curves tracking the conductivity of barite growth solutions (S = 10) at ambient temperature (21.0 ± 0.5 °C) during bulk assay synthesis in the presence of various alginate concentrations. A linear regression is performed on the first 40 min of each experiment to report the depletion rate of growth solutes from the bulk.

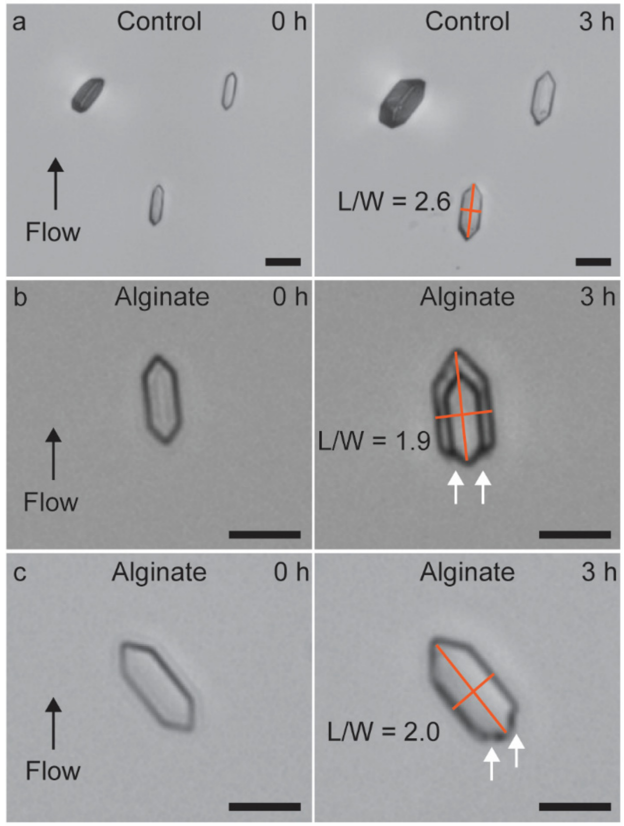

Figure S8. Time-resolved optical micrographs of seed crystals exposed to flow (12 mL h^{-1}) of supersaturated growth solutions (S = 7) in: (a) the absence of alginate, (b) the presence of 0.03 µg mL^{-1} alginate, and (c) 0.1 µg mL^{-1} alginate. Crystals with aspect ratios (length/width) below a value of 2.0 were evaluated for features induced by flow as indicated in the white arrows and were subsequently categorized as "crystals affected by direction of flow". Scale bars equal 20 µm. A minimum of 100 crystals per experiment were analyzed over 3 separate experiments.

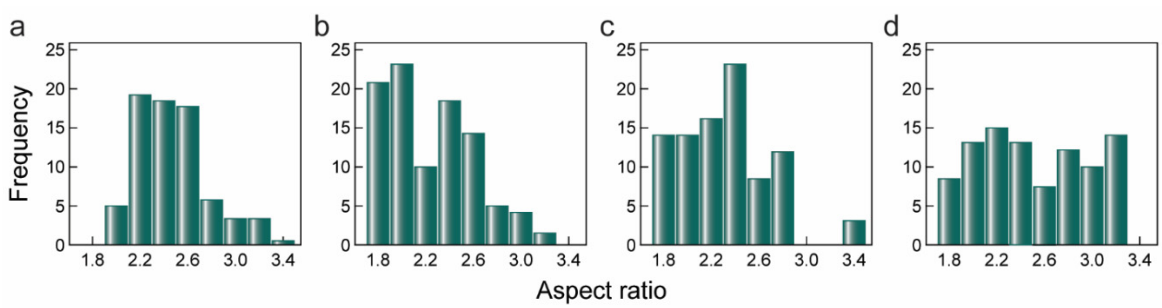

Figure S9. Aspect ratio measurements for crystals grown in microchannels under flow (12 mL h^{-1}) of supersaturated solutions (S = 7) containing Ba^{2+} and SO_4^{2-} ions and alginate concentrations of (a) 0 (b) 0.03 (c) 0.05, and (d) 1.0 µg mL^{-1} at pH 7. The control in (a) has few crystals with aspect ratios less than 2.4, whereas the frequency of smaller aspect ratios is higher in the presence of alginate. Histograms depict the number of crystals in microchannels as a function of aspect ratio for individual trials at each alginate concentration. A minimum of 100 crystals were measured for separate experiments at each alginate concentration.

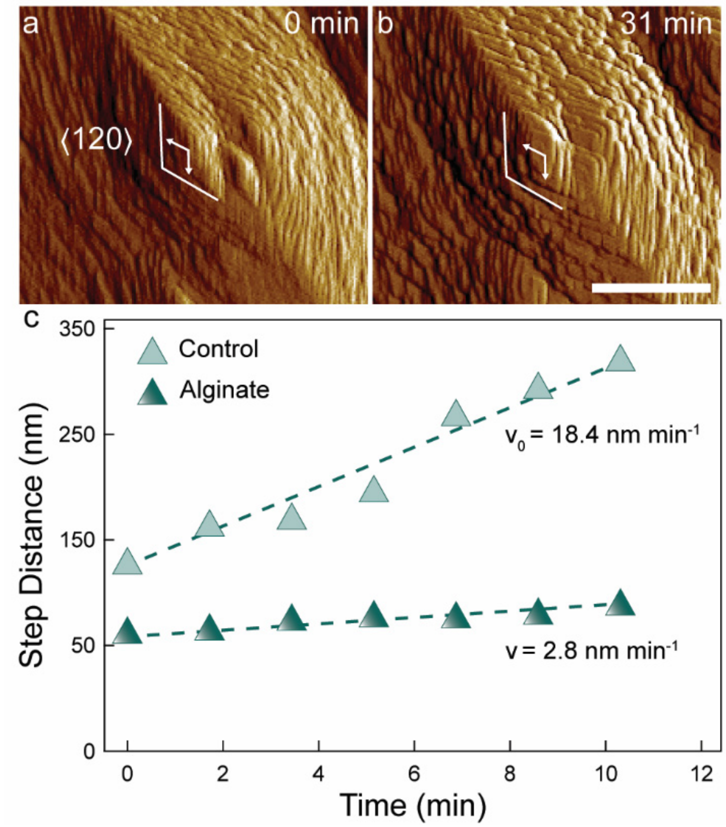

Figure S10. (a) - (b) In situ atomic force microscopy images extracted from Movie S2 showing the step advancement of a growth hillock on a (001) barite surface under flow of a growth solution (S = 4.4) in the presence of 1 µg mL^{-1} alginate. Scale bar equals 500 nm. (c) Measurements of single step advancement in the absence and presence of 1 µg mL^{-1} alginate, representative of the AFM data analysis for all in situ experiments. Symbols represent the distance between the [120] step-front and the central point of the growth hillock as a function of time. Dashed lines are linear fits, where the slopes (v_0 and v) indicate step velocities in the absence and presence of 1 µg mL^{-1} alginate, respectively. A minimum of 10 step fronts were analyzed in this fashion for each concentration. Three separate experiments were performed for each concentration.

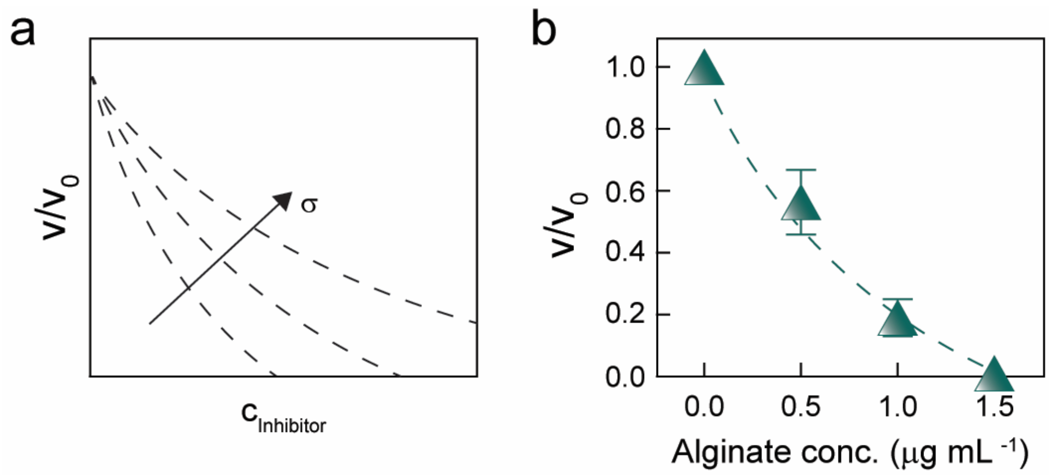

Figure S11. (a) Theoretical Cabrera-Vermilyea (CV) curves[1, 2] for crystal inhibitors that follow a step-pinning mode of action as a function of increasing growth solution relative supersaturation σ. (b) Step velocity in the $\langle 120 \rangle$ direction for growth solutions containing alginate relative to those without any additive (control) as a function of increasing alginate concentration. Data points denote the average of at least 3 separate experiments. Error bars span two standard deviations and the dashed line is interpolated to guide the eye. The monotonic decrease in relative step velocity with increasing inhibitor concentration mirrors the trend in the theoretical CV curves in (a) suggesting a step-pinning mode of action of alginate on the barite (001) surface.

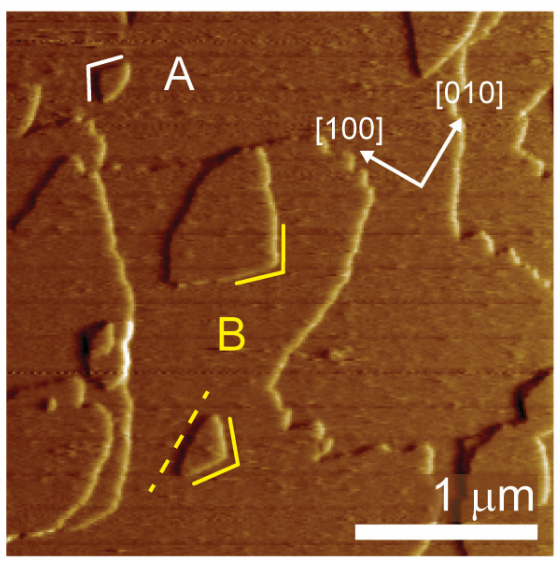

Figure S12. *In situ* atomic force microscopy deflection mode image extracted from Movie S3 showing the birth and spread of 2D nuclei on the (001) barite surface. Annotations demonstrate examples of a 180° inversion of 2D nuclei orientation. "A" denotes the layer that generates 2D nuclei (examples labeled in white boundaries) oriented in the [100] direction, while "B" denotes the layer that produces 2D nuclei (examples labeled in yellow boundaries) oriented in the [$\bar{1}$00] direction. The yellow dashed line indicates the axis of inversion of 2D islands.

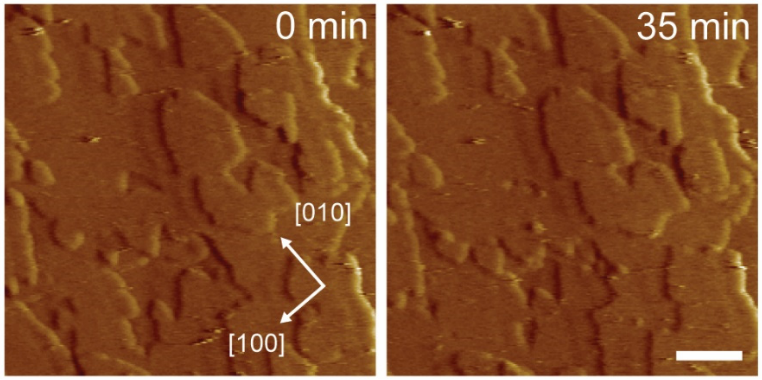

Figure S13. Time-resolved *in situ* atomic force microscopy images showing the suppression of step advancement of 2D layers on a (001) barite surface under flow of a growth solution (S = 5.3) containing Ba^{2+}, SO_4^{2-}, and 1 μg mL^{-1} alginate. Scale bar equals 500 nm.

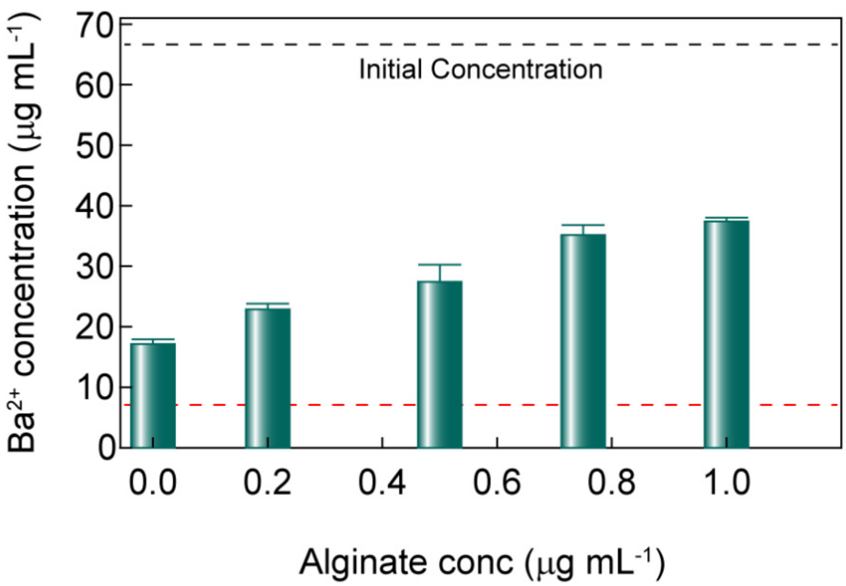

Figure S14. Elemental analysis (ICP-OES) of free Ba^{2+} ion concentration in the supernatant after a 24 synthesis from bulk assays as a function of concentration. The grey dashed line indicates initial Ba^{2+} ion concentration (S = 10). The red dashed line corresponds to the solubility, C_e, of barite at 25 °C.[3] A monotonic increase in Ba^{2+} concentration with increasing alginate concentration indicates the latter leads to a more metastable solution (i.e. higher supersaturation) by suppressing barite crystallization and potentially sequestering free Ba^{2+} ions in solution. A minimum of 3 batches were analyzed for each concentration. Error bars equal one standard deviation.

Supplementary Movies

Movie S1. Time-elapsed sequence of brightfield optical images showing the growth of barite seed crystals in microchannels under flow of a supersaturated (S = 7) solution containing Ba^{2+} and SO_4^{2-} ions, and 0.03 μg mL^{-1} alginate. Inhibition on barite crystal surfaces depends on the flow orientation, resulting in anisotropic growth and preferential suppression of facets directly facing the oncoming flow. The total imaging time for the *in situ* optical microscopy video is 3 h.

Movie S2. Time-elapsed sequence of AFM deflection mode images depicting the spiral growth of the (001) barite surface in a supersaturated (S = 4.4) solution containing only Ba^{2+} and SO_4^{2-} ions, followed by a reduction in the step velocities when the flowing solution is switched to a supersaturated solution containing Ba^{2+} and SO_4^{2-} ions with alginate. The growth solutions were introduced at a flow rate of 12 mL h^{-1}. The spiral growth hillock displays a diamond morphology bound by the [120] directions. The height of each layer corresponds to the dimension of a half unit cell in the c-direction (*c/2*). The total imaging time for the *in situ* AFM video is 63 min.

Movie S3. Time-elapsed sequence of AFM deflection mode images depicting the growth of a (001) barite surface in a supersaturated (S = 5.3) solution followed by the suppression of step advancement when the flowing solution is switched to a supersaturated solution containing Ba^{2+} and SO_4^{2-} ions with alginate. The growth solutions were introduced at a flow rate of 12 mL h^{-1}. The (001) surface becomes populated with triangular 2-D layers with a morphology bound by the [010] and [120] directions that advance laterally in the pure growth solution. The height of each layer corresponds to the dimension of a half unit cell in the c-direction (*c/2*). Upon introducing the growth solution containing alginate, 2-D layer advancement is suppressed resulting in step bunching. The total imaging time for the *in situ* AFM video is 64.7 min.

References

1. Wang, L., J.J. De Yoreo, X. Guan, S.R. Qiu, J.R. Hoyer, and G.H. Nancollas, *Constant composition studies verify the utility of the Cabrera− Vermilyea (CV) model in explaining mechanisms of calcium oxalate monohydrate crystallization.* Crystal Growth & Design, 2006. **6**: 1769-1775.

2. Cabrera, N., D. Vermilyea, R. Doremus, B. Roberts, and D. Turnbull, *Growth and perfection of crystals.* 1958. **393**.

3. Blount, C.W., *Barite solubilities and thermodynamic quantities up to 300 C and 1400 bars.* American Mineralogist, 1977. **62**: 942-957.